Measurement of the linear electro-optic tensor of cubic boron nitride single crystals

Shuang Wang (王 爽)[1], Gang Jia (贾 刚)[1], Xiuhuan Liu (刘秀环)[2], Shipeng Chi (迟世鹏)[1], Jingcheng Zhu (朱景程)[1], Yanjun Gao (高延军)[1], Pingwei Zhou (周平伟)[1], and Zhanguo Chen (陈占国)[1*]

[1] *State Key Laboratory on Integrated Optoelectronics, College of Electronic Science and Engineering, Jilin University, Changchun 130012, China*

[2] *College of Communication Engineering, Jilin University, Changchun 130012, China*

[*] *Corresponding author: czg@jlu.edu.cn*

Received September 16, 2011; accepted November 7, 2011; posted online January 6, 2012

The transverse electro-optic (EO) modulation system is built based on cubic boron nitride (cBN) single crystals unintentionally doped and synthesized at a high pressure and high temperature. The photoelectric output of the system includes two parts that can be measured respectively and the value of elements in the linear EO tensor of the cBN crystal can be obtained. This method does not need to measure the absolute light intensity. All of the surfaces of the tiny cBN crystals whose hardness is next to the hardest diamonds are {111} planes. The rectangular parallelepiped cBN samples are obtained by cleaving along {110} planes and subsequently grinding and polishing {112} planes of the tiny octahedral cBN flakes. Three identical non-zero elements of the EO tensor of the cBN crystal are measured via two sample configurations, and the measured results are very close, about 3.68 and 3.95 pm/V, respectively, which are larger than the linear EO coefficients of the general III-V compounds.

OCIS codes: 160.2100, 160.4760, 190.4400, 190.4720.
doi: 10.3788/COL201210.041602.

Cubic boron nitride (cBN) has a zinc blend structure and belongs to the T_d point group; thus, it possesses the linear electro-optic (EO) effect. Its EO tensor possesses only three identical non-zero elements, namely, $\gamma_{41} = \gamma_{52} = \gamma_{63}$. The bandgap of cBN is about 6.3 eV[1−3], which is the widest among the III-V compounds. Therefore, cBN is transparent in throughout the visible range and most of the infrared and ultraviolet spectra; it can also operate in the wide spectral range as the EO material. Furthermore, cBN has a very high laser damage threshold, meaning it can withstand high-power pulsed or continuous-wave (CW) laser beams. Thus, cBN has potential EO applications. The determination of the EO coefficients of cBN crystals is a prerequisite not only for the EO applications, but also for other studies (e.g., for the study of Raman efficiency of cBN[4] and for the propagation control of the surface wave generated from the interface between the cBN crystal and other isotropic medium[5]). Some different theoretical results of the EO tensor of the cBN crystals have been reported[6−8], but these results were only evaluated based on the second-order non-linear susceptibility $\chi^{(2)}(-2\omega,\ \omega,\ \omega)$, which is related to the second harmonic generation. In fact, the linear EO coefficient $\gamma_{41}(\omega)$ should be obtained based on $\chi^{(2)}(-\omega,\ \omega,\ 0)$, which is relevant to the linear EO effect and optical rectification. Because of the frequency dispersion of the second-order non-linear susceptibility, $\chi^{(2)}(-2\omega,\ \omega,\ \omega) \neq \chi^{(2)}(-\omega,\ \omega,\ 0)$; that is, the accurate value of $\gamma_{41}(\omega)$ should come from the experiments of the linear EO effect or optical rectification. Unfortunately, very few reports[9] have yet examined the experimental value of γ_{41} of cBN crystals. The main obstacles may include the difficulties of synthesizing the high-quality large cBN crystals and fabricating cBN crystals into suitable rectangular parallelepiped samples because of the second highest hardness. The cBN sample used in Ref. [9] was an irregular octahedral crude flake whose entire surfaces were {111} planes. The experimental system was different from the conventional transverse EO modulator. The refraction took place twice when the probing beam passed the cBN flake. The signal-to-noise ratio (SNR) was lower because of the larger loss from the reflection and diffraction. Consequently, the result had a larger error.

In this letter, rectangular parallelepiped cBN samples were obtained from some tiny octahedral cBN flakes using mechanical cleavage, grinding, and polishing, and a transverse EO modulation system based on these cBN samples was built to investigate the linear EO effect and accordingly measure the experimental value of γ_{41} of cBN crystals.

The unintentionally doped cBN crystals used in our experiments were synthesized at a high pressure and high temperature; these were originally octahedral flakes, as shown in Fig. 1(a). All the surfaces of the octahedral cBN flake are {111} planes, among which the two larger parallel planes are denoted as (111) and $(\bar{1}\bar{1}\bar{1})$ planes; each pair of opposite planes are also parallel in the

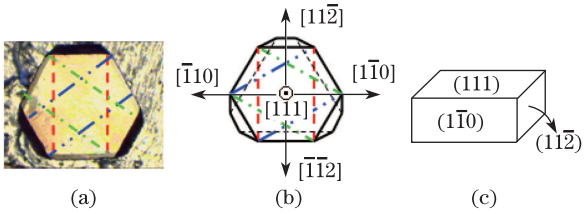

Fig. 1. Schematic diagrams of the cBN crystals used in experiments. (a) Micrograph of the actual cBN crystal; (b) directions for the cleavage surfaces of the cBN crystal; (c) rectangular parallelepiped cBN sample.

 © 2012 Chinese Optics Letters

other six {111} planes. Since the cleavage planes of cBN crystals are {110} planes due to the zinc blende structure[10], there are three kinds of possible cleavage fracture surfaces perpendicular to (111) and $(\bar{1}\bar{1}\bar{1})$ planes, as shown in Figs. 1(a) and (b) and marked as $(1\bar{1}0)$ or $(\bar{1}10)$ planes, $(\bar{1}01)$ or $(10\bar{1})$ planes, and $(0\bar{1}1)$ or $(01\bar{1})$ planes, respectively. In our experiments, we cleaved the cBN flake along the $[11\bar{2}]$ direction, resulting in $(1\bar{1}0)$ and $(\bar{1}10)$ fracture surfaces. The rectangular parallelepiped cBN sample is schematically shown in Fig. 1(c). $(11\bar{2})$ and $(\bar{1}\bar{1}2)$ planes perpendicular to both (111) and $(1\bar{1}0)$ planes were obtained by grinding and polishing with diamond powder.

The rectangular parallelepiped cBN samples are so tiny that the sample holder must be specially designed and fabricated. The configuration of the sample holder is schematically shown in Fig. 2. Two chamfered glass slides (shown in Fig. 2(b)), on to which aluminum foil was stuck as the electrodes, were used for clamping the cBN sample, and the gap between the two slides were sealed with opaque black insulating glue to ensure that only the light propagating through the cBN sample could be detected.

Without the electric field, a cBN crystal is optically isotropic. However, it can turn into a birefringent crystal using the applied electric field. As for the cBN sample, the electric field can be applied perpendicularly to (111), $(1\bar{1}0)$, and $(11\bar{2})$ planes. In the principle coordinates—namely, the directions of [100], [010], and [001] are along the x, y, and z axes, respectively—the principle indices and other relevant parameters of cBN dependent on the applied electric field (or the applied voltage) can be deduced by solving the refractive index ellipsoid equations. The results are summarized in Table 1.

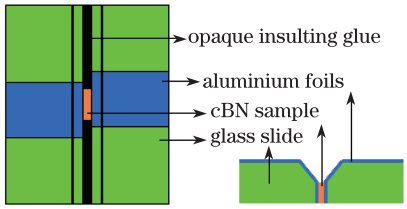

Fig. 2. Configuration of the cBN sample holder. (a) Top view; (b) sectional view.

Table 1. Birefringence Induced by the Electric Fields Applied along Different Directions in cBN Crystals

E	$E\perp$ (111) Plane $E_x = E_y = E_z = \frac{E}{\sqrt{3}}$	$E\perp(1\bar{1}0)$ Plane $E_x = -E_y = \frac{E}{\sqrt{2}}, E_z = 0$	$E\perp(11\bar{2})$ Plane $E_x = E_y = \frac{\sqrt{6}}{6}E, E_z = -\frac{\sqrt{6}}{3}E$
Index Ellipsoid	$(x^2+y^2+z^2)/n_0^2$ $+\frac{2}{\sqrt{3}}\gamma_{41}E\,(yz+zx+xy) = 1$	$(x^2+y^2+z^2)/n_0^2$ $+\sqrt{2}\gamma_{41}E(yz-zx) = 1$	$(x^2+y^2+z^2)/n_0^2$ $+\frac{\sqrt{6}}{3}\gamma_{41}E\,(yz+zx-2xy) = 1$
$n_{x'}$	$n_0 + n_0^3\gamma_{41}E/2\sqrt{3}$	$n_0 - n_0^3\gamma_{41}E/2$	$n_0 + (3\sqrt{2}+\sqrt{6})n_0^3\gamma_{41}E/12$
$n_{y'}$	$n_0 + n_0^3\gamma_{41}E/2\sqrt{3}$	$n_0 + n_0^3\gamma_{41}E/2$	$n_0 - (3\sqrt{2}-\sqrt{6})n_0^3\gamma_{41}E/12$
$n_{z'}$	$n_0 - n_0^3\gamma_{41}E/2\sqrt{3}$	n_0	$n_0 - n_0^3\gamma_{41}E/\sqrt{6}$
xyz and $x'y'z'$ Coordinate	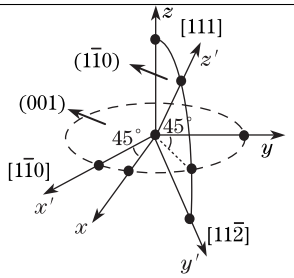	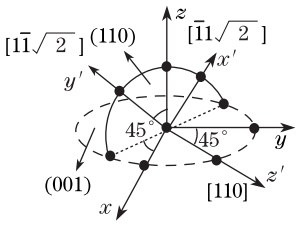	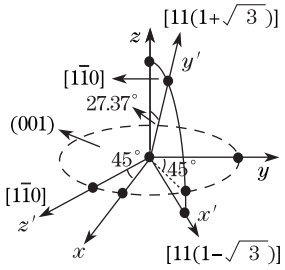
Directions of Optical Path and Axes of Crossed Polarizer	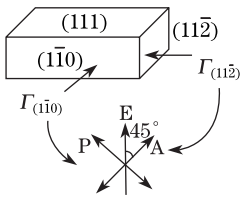	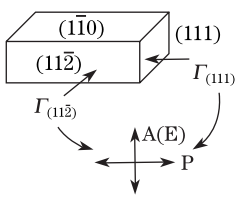	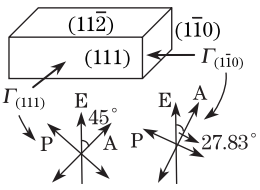
Phase Difference Γ ($V = Ed$)	$\Gamma_{[1\bar{1}0]} = \Gamma_{[11\bar{2}]}$ $=\sqrt{3}\pi n_0^3\gamma_{41}Vl/\lambda d$	$\Gamma_{[111]} = 2\sqrt{6}\pi n_0^3\gamma_{41}Vl/3\lambda d$ $\Gamma_{[11\bar{2}]} = 2\sqrt{3}\pi n_0^3\gamma_{41}Vl/3\lambda d$	$\Gamma_{[111]} = 2\sqrt{6}\pi n_0^3\gamma_{41}Vl/3\lambda d$ $\Gamma_{[1\bar{1}0]} = \sqrt{30}\pi n_0^3\gamma_{41}Vl/3\lambda d$
Half-Wave Voltage V_π	$V_{\pi[1\bar{1}0]} = V_{\pi[11\bar{2}]}$ $= \lambda d/\sqrt{3}n_0^3\gamma_{41}l$	$V_{\pi[111]} = \sqrt{6}\lambda d/4n_0^3\gamma_{41}l$ $V_\pi[11\bar{2}] = \sqrt{3}\lambda d/2n_0^3\gamma_{41}l$	$V^{=}_{\pi[111]}\sqrt{6}\lambda d/4n_0^3\gamma_{41}l$ $V^{=}_{\pi[1\bar{1}0]}\sqrt{30}\lambda d/10n_0^3\gamma_{41}l$

n_0=2.117[11] is the isotropic index of cBN; γ_{41} is one of three identical non-zero elements of the EO tensor of cBN; V is the applied voltage to the cBN sample; E is the applied electric field; d is the distance between the two parallel planar electrodes; l is the length of the probing beam propagating through the sample.

According to these results, the transverse EO modulation system for measuring the linear EO coefficient of cBN was built, as shown in Fig. 3. The system is similar to the one for measuring the third-order nonlinear optical susceptibility of synthetic diamonds[12], but the focusing lenses are unnecessary because the light intensity through the cBN sample is strong enough. The light source is a CW semiconductor laser with the wavelength $\lambda = 650$ nm. The polarization of the polarizer is horizontal, which is orthogonal to that of the analyzer. The fast (or slow) axis of the quarter wave plate is 45° with respect to the polarization of the polarizer. The two eigenpolarizations of the modulated cBN sample are parallel to the fast (or slow) axis of the quarter wave plate. The output beam from the sample is elliptically polarized. The intensity of the output beam from the analyzer $I_{\rm o}$ is dependent on the phase difference Γ, namely

$$\begin{aligned} I_{\rm o} &= I_{\rm i}\left(1+\sin\Gamma\right)/2 \approx I_{\rm i}\left(1+\Gamma\right)/2 \\ &= I_{\rm i}\left(1+\pi V_{\rm m}/V_\pi\right)/2 = I_1 + I_2, \end{aligned} \tag{1}$$

where $I_{\rm i}$ is the intensity of the input beam, $\Gamma = \pi V_{\rm m}/V_\pi << 1$ is the phase difference between the two eigenpolarization rays induced by the modulating voltage $V_{\rm m}$[13], and V_π is the half-wave voltage relevant to the refractive index, the linear EO coefficient, and the size of the sample, just like the expressions in Table 1. In addition, according to Eq. (1), $I_1 = I_{\rm i}/2$ is independent of the modulating voltages $V_{\rm m}$, whereas $I_2 = \pi I_{\rm i} V_{\rm m}/2V_\pi$ is apparently dependent on $V_{\rm m}$. I_1 and I_2 can be detected using the Si photodetector connected with the lock-in amplifier.

First, without the modulating voltage, the photoelectric signal U_1 induced by I_1 was measured when the chopper operated at 143 Hz. U_1 can be written as

$$U_1 = 2MI_1/\pi = MI_i/\pi, \tag{2}$$

where $2/\pi$ is the modified factor due to the Fourier transformation of the square wave and M is a constant coefficient related to the measuring system, such as the optical elements, the responsivity of the Si photodetector, and the electronic instruments.

Next, without the chopper, the photoelectric signal U_2 induced by I_2 was measured when the modulating voltage $\widetilde{V} = V_{\rm m}\sin\omega_{\rm m}t$ is applied to the cBN sample. The modulating frequency was set to $\omega_{\rm m}$=143 Hz, while other measuring conditions were maintained the same as those

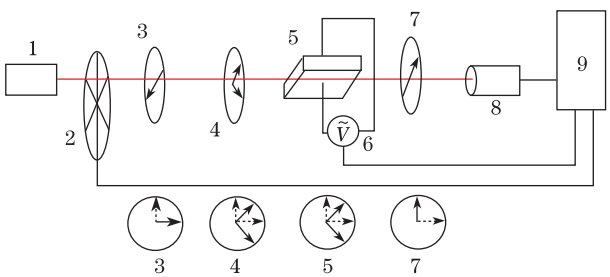

Fig. 3. Transverse EO modulation system for measuring the EO coefficient of cBN single crystal. 1. 650-nm laser; 2. chopper; 3. polarizer; 4. quarter wave plate; 5. cBN sample; 6. signal generator; 7. analyzer; 8. Si photodetector; 9. lock-in amplifier.

in the process of measuring U_1. Thus, U_2 can be expressed as

$$U_2 = MI_2 = MI_{\rm i}\pi V_{\rm m}/2V_\pi. \tag{3}$$

In experiments, the dependence of U_2 on the effective value (root mean square value) of the sinusoidal modulating voltage $V_{\rm eff} = V_{\rm m}/\sqrt{2}$ was measured. According to Eq. (3), U_2 should be proportional to $V_{\rm eff}$. As a result, the ratio k can be deduced as

$$k = U_2/V_{\rm eff} = \pi M I_{\rm i}/\sqrt{2}V_\pi, \tag{4}$$

which is also the slope of the experimental line of U_2 compared to $V_{\rm eff}$ and can be feasible to obtain. Based on the experimental values of k and U_1, the half-wave voltage V_π can be calculated using Eqs. (2) and (4). The relationship between the half-wave voltage V_π and the linear EO coefficient γ_{41} is described in Table 1. The sizes of the cBN sample, l and d, were measured using a metalloscope; thus, the linear EO coefficient γ_{41} of the cBN crystal can be determined at last.

According to the theoretical analysis summarized in Table 1, three configurations of the cBN sample are possible. After adjusting the intensity of the input beam and making the value of U_1 be 0.53 mV in experiments, the detailed experimental processes and results are as follows:

(i) The electric field was applied along the [111] axis of the cBN sample. In this instance, the cBN sample became a uniaxial crystal, and the optical axis was just the [111] axis. The light was allowed to propagate perpendicularly to the [111] direction. In our cBN samples, the cleavage surface $(1\bar{1}0)$ was smoother than the $(11\bar{2})$ plane, so the probing beam perpendicularly irradiated the $(1\bar{1}0)$ plane. A good linear relationship was measured between U_2 and $V_{\rm eff}$, as shown in Fig. 4. The slope $k = 7.25\times10^{-7}$ can be obtained from Fig. 4. Based on Eqs. (2) and (4), the half-wave voltage $V_\pi = 5.10\times10^3$ V can be calculated. The sizes of the cBN sample 1, $l = 324.25$ μm, and $d = 154.08$ μm, were measured. From $V_\pi = \lambda d/\sqrt{3}n_0^3\gamma_{41}l$ (as shown in Table 1), the linear EO coefficient γ_{41}=3.68 pm/V was calculated.

(ii) The electric field was applied along the $[1\bar{1}0]$ axis of the cBN sample. In this case, the cBN sample became a biaxial crystal, and the principal axes of the index ellipsoid were $[\bar{1}1\sqrt{2}]$, $[1\bar{1}\sqrt{2}]$, and [110], respectively. The first and second principal axes were not the usual crystal orientations, and their z-components were irrationals. However, the outside surfaces of the cBN sample did not include $(\bar{1}1\sqrt{2})$, $(1\bar{1}\sqrt{2})$, or (110) planes. The (111) plane of the cBN sample was selected as the perpendicularly incident surface of the probing beam because it was bigger and smoother than the $(11\bar{2})$ plane.

The birefringence also occurred in the sample. The two eigenpolarization modes and the phase difference between them can be deduced from the theory of the index ellipsoid as well, as shown in the third column of Table 1. The relationship between U_2 and $V_{\rm eff}$ was measured too, as shown in Fig. 5. It is a perfect line. The slope $k = 1.65\times10^{-7}$ was obtained, so $V_\pi = 2.24\times10^4$ V.

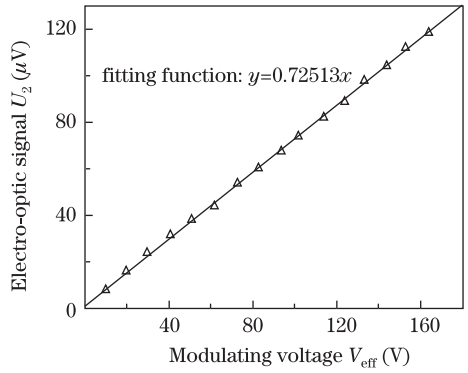

Fig. 4. EO signal U_2 versus the modulating voltage $V_{\rm eff}$ for the first sample configuration.

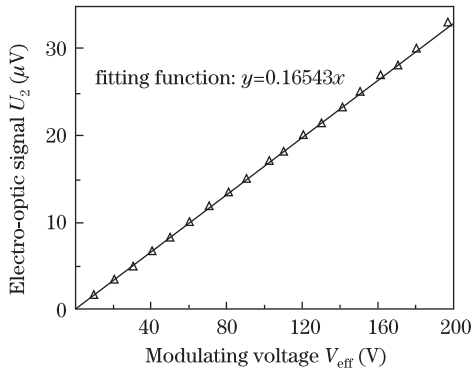

Fig. 5. EO signal U_2 versus the modulating voltage $V_{\rm eff}$ for the second sample configuration.

The size of the cBN sample 2, l = 149.44 μm and d = 314.47 μm, was measured. According to $V_\pi = \sqrt{6}\lambda d/\,4n_0^3\gamma_{41}l$, the linear EO coefficient γ_{41}=3.95 pm/V was finally obtained.

(iii) The electric field was applied along the $[11\bar{2}]$ axis of the sample. In this situation, the cBN sample became a biaxial crystal as well, and the eigenvectors of the three principal axes of the index ellipsoid were $[11(1-\sqrt{3})]$, $[11(1+\sqrt{3})]$, $[1\bar{1}0]$ {←insert and before third factor}. The first two eigenvectors are not the usual crystal orientations, and their z-components were irrationals. We did not adopt this sample configuration for the following reasons. (a) The distance between two parallel electrodes (or the $(11\bar{2})$ and $(\bar{1}\bar{1}2)$ planes) is much larger than the light path of the probing beam in the sample–namely, the ratio of d/l is large–so the half-wave voltage is high and the voltage sensitivity of the measuring system is low; (b) although the distance between the electrodes can be shortened by grinding and polishing, the diffraction will become more severe because of the tinier incident surface of the sample; (c) the $(11\bar{2})$ and $(\bar{1}\bar{1}2)$ planes are small, but the distance between them is large; consequently, if the electrodes are applied to them, the leakage loss of the electric field will become serious and induce severe measuring errors.

In our experiments, the possible measuring errors include the followings aspects. Firstly, because the cBN crystal turns into a uniaxial or biaxial crystal under the applied electric field, the walk-off effect of the output light from the sample occurs when the light does not propagate along the principal axis. However, the modulating electric field was so weak in experiments that the walk-off effect was ignored. Secondly, due to the distortion of the electric field at the edges of the electrodes, the actual field strength was lower than the calculated uniform electric field value, which made the experimental result γ_{41} smaller than the actual one. Third, U_1 and U_2 are not measured simultaneously, and the fluctuations of the light source may result in errors. Therefore, a comparatively stable semiconductor laser was used during the experiments. Finally, the incident surface of the sample is small, resulting in the diffraction effect. This phenomenon was more considerable in the first sample configuration than in the second one. The diffraction can decrease the measured value of U_2 since the diffractive light cannot perpendicularly go through the analyzer. This is also one of the reasons why the measured linear EO coefficient γ_{41} was smaller in the first sample configuration than in the second one. Shortening the distance between the sample and the analyzer can reduce the effect of the diffraction. In fact, the two measured values of γ_{41} have the same order of magnitude, and the relative error between them is only about 7%, which also indicates that the measuring system and method are both very credible.

The linear EO coefficient $\gamma_{ijk}(\omega)$ is connected to the second-order optic susceptibility $\chi^{(2)}_{ijk}(-\omega,\omega,0)$ through the relation[14]

$$\gamma_{ijk}(\omega) = -2\chi^{(2)}_{ijk}(-\omega,\omega,0)/\varepsilon_{ii}\varepsilon_{jj}, \tag{5}$$

where ε is the dielectric constant of cBN crystals at the frequency ω. However, most theoretical calculations can only give the value of $\chi^{(2)}(-2\omega,\ \omega,\ \omega)$. In the zero frequency limit[8], we have

$$\lim_{\omega\to 0}\chi^{(2)}_{ijk}(-2\omega,\omega,\omega) = \lim_{\omega\to 0}\chi^{(2)}_{ijk}(-\omega,\omega,0)\,. \tag{6}$$

Thus, only $\gamma_{ijk}(0)$ can be deduced from the theoretical value of $\chi^{(2)}(-2\omega,\omega,\omega)$. However, this method neglects the dispersion characteristic of the EO coefficients; in fact, $\gamma_{ijk}(0) \neq \gamma_{ijk}(\omega)$. Applying this method, the calculated γ_{41} of the cBN crystal is about 0.10 pm/V[6], the calculated EO coefficients of the isolated BN sheet and BN nanotube (17, 0) are $\gamma_{22} = -1.78$, $\gamma_{12} = 1.78$[8], $\gamma_{13} = -2.08$, $\gamma_{51} = -2.11$, and $\gamma_{33} = 3.53$[8], respectively. These theoretical values are all less than the measured values of 3.68 and 3.95 pm/V. Moreover, the measured γ_{41} of the cBN crystal is also larger than the linear EO coefficients of GaN[15], AlN[16], GaP, and GaAs. These EO coefficients are listed and compared in Table 2.

In conclusion, based on the tiny rectangular parallelepiped cBN sample manufactured by physically cleaving and mechanically grinding and polishing, a transverse EO modulation system is built up. Applying two sample configurations, three identical non-zero elements of the EO tensor of the cBN crystal $\gamma_{41} = \gamma_{52} = \gamma_{63}$ are experimentally measured according to the ratio of the two components (one component depends on the modulating voltage whereas the other does not) of the output beams. The measured results indicate that cBN crystals are

Table 2. EO Coefficients of Some III-V Compounds at Room Temperature

Materials	Symmetry	EO Coefficients (pm/V)
cBN	T_d	$\gamma_{41} = 3.68/3.95$, $\gamma_{41} = 0.10$[6]
AlN	C_{6V}	$\gamma_{13} = 0.67, \gamma_{33} = -0.59$[16]
GaN	C_{6V}	$\gamma_{13} = 0.57 \pm 0.11, \gamma_{33} = 1.91 \pm 0.35$[15]
GaP	T_d	$\gamma_{41} = 0.97$[14]
GaAs	T_d	$\gamma_{41} = 1.6$[14]

very promising EO material. In addition, the measuring method of the linear EO coefficient adopted in this letter is very convenient and feasible as it is unnecessary to measure the absolute intensity of the probing beam.

This work was supported by the National Natural Science Foundation of China (Nos. 60976037 and 61077026), the Joint Research Project of NSFC-RFBR (No. 61111120097), and the National High-Technology Research and Development Program of China (No. 2009AA03Z419).

References

1. O. Mishima and K. Era, *Electric Refractory Materials* Y. Kumashiro (eds.) (Marcel Dekker, New York, 2000) p. 495.
2. P. Rodríguez-Hernández, M. González-Diaz, and A. Muñoz, Phys. Rev. B **51,** 14705 (1995).
3. T. Taniguchi, K. Watanabe, S. Koizumi, I. Sakaguchi, T. Sekiguchi, and S. Yamaoka, Appl. Phys. Lett. **81,** 4145 (2002).
4. S. Reich, A. C. Ferrari, R. Arenal, A. Loiseau, I. Bello, and J. Robertson, Phys. Rev. B **71,** 205201 (2005).
5. S. R. Nelatury, J. A. Polo, and A. Lakhtakia, Electromagnetics **28,** 162 (2008).
6. V. I. Gavrilenko and R. Q. Wu, Phys. Rev. B **61,** 2632 (2000).
7. J. Chen, L. Jönsson, J. W. Wilkins, and Z. H. Levine, Phys. Rev. B **56,** 1787 (1997).
8. G. Guo and J. Lin, Phys. Rev. B **72,** 075416 (2005)[Erratum: Phys. Rev. B **77,** 049901(E) (2008)].
9. K. Cao, Z. Chen, C. Ren, G. Jia, T. Zhang, X. Liu, B. Shi, and J. Zhao, Microelectronics J. **40,** 70 (2009).
10. S. Yang, Z. Wang, and J. Wang, *Semiconductor Materials* (in Chinese) (Jilin University, Changchun, 1997).
11. T. Zhang and G. Zou, *Cubic Boron Nitride* (in Chinese) (Jilin University, Changchun, 1993).
12. J. Zhao, G. Jia, X. Liu, Z. Chen, J. Tang, and S. Wang, Chin. Opt. Lett. **8,** 685 (2010).
13. A. Yariv, *Introduction to Optical* (in Chinese) (Science, Beijing, 1983).
14. S. Shi, G. Chen, W. Zhao, and J. Liu, *Nonlinear Optics* (in Chinese) (Xi'an University, Xi'an, 2003).
15. X.-C. Long, R. A. Myers, S. R. J. Brueck, R. Ramer, K. Zheng, and S. D. Hersee, Appl. Phys. Lett. **67,** 1349 (1995).
16. P. Gräupner, J. C. Pommier, A. Cachard, and J. L. Coutaz, J. Appl. Phys. **71,** 4136 (1992).